Electronic Supplementary Material (ESI) for Journal of Materials Chemistry A.

Safely probing the chemistry of Chernobyl nuclear fuel using micro-focus X-ray analysis: Supplementary Material

Hao Ding[1], Malin C. Dixon Wilkins[1], Clémence Gausse[1], Lucy M. Mottram[1], Shikuan Sun[1], Martin C. Stennett[1], Daniel Grolimund[2], Ryan Tappero[3], Sarah Nicholas[3], Neil C. Hyatt[1*] and Claire L. Corkhill[1*]

[1]NucleUS Immobilisation Science Laboratory, Department of Materials Science and Engineering, The University of Sheffield, S1 3JD, UK.

[2]Swiss Light Source, Paul Scherrer Institut, 5232 Villigen PSI, Switzerland

[3]Brookhaven National Laboratory, NSLS-II, Upton, NY, 11973, USA

*corresponding authors: c.corkhill@sheffield.ac.uk; n.c.hyatt@sheffield.ac.uk

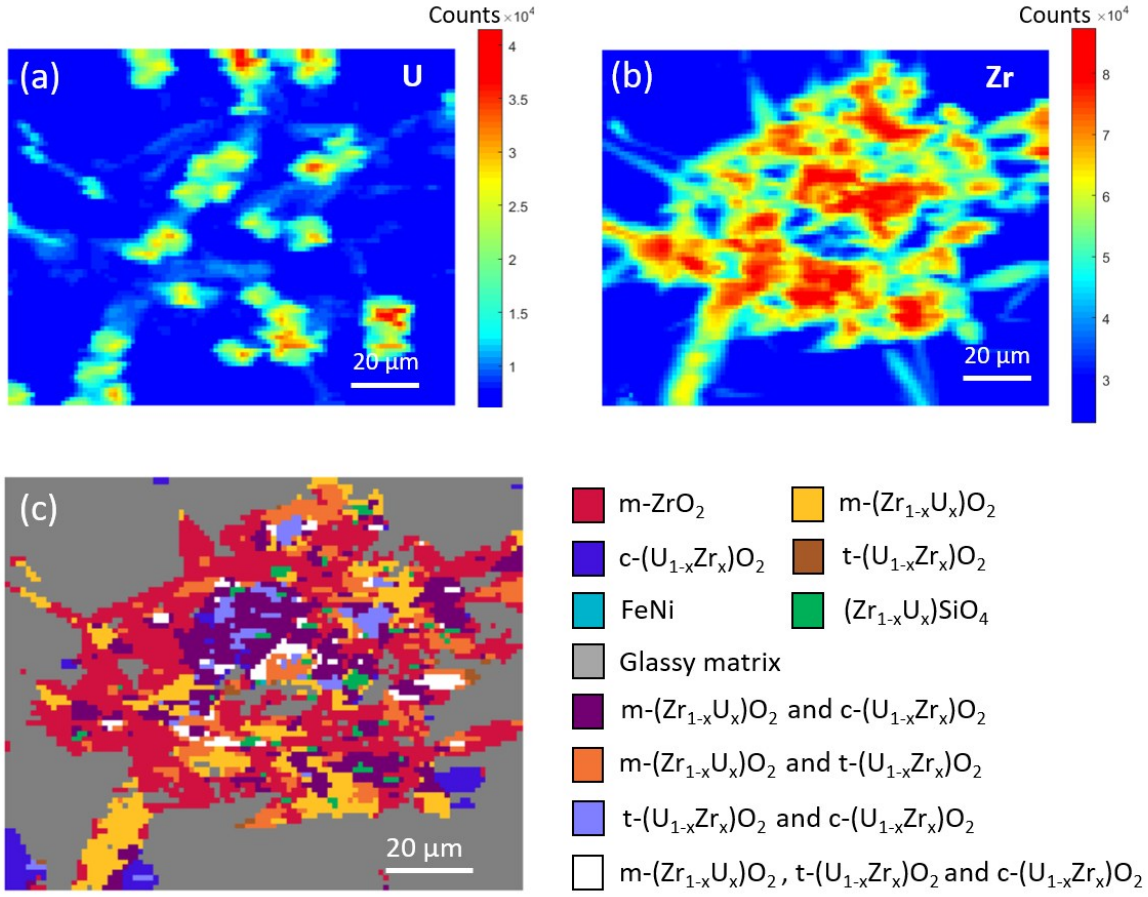

Supplementary Figure 1. Black LFCM agglomerate with radiating dendrites, showing **a** U-Lα and **b** Zr-Kα and **c** 2D µ-diffraction map reconstructed from XRD patterns. This more agglomerated particle was made up of many fused particles in the centre, surrounded by several dendrites. The full range of U-Zr-O crystallites, including c-$(U_{0.9}Zr_{0.1})O_2$, t-$U_{0.1}Zr_{0.9}O_2$, m-$(Zr_{1-x}U_x)O_2$ and ZrO_2, were identified. The formation of this morphology and the variations of composition are postulated to be the result of centrally crystallised c-$(U_{1-x}Zr_x)O_2$ clusters reacting with m-ZrO_2. One very small Fe-Ni inclusion was encapsulated within the centre of the agglomerate, and several small zircon particles (2µm - 8µm) were observed around the edge, or within cracks, of the agglomerates, where they contacted the glass matrix. This suggests that the formation of zircon took place at the interface between the inclusions and the glass phase.

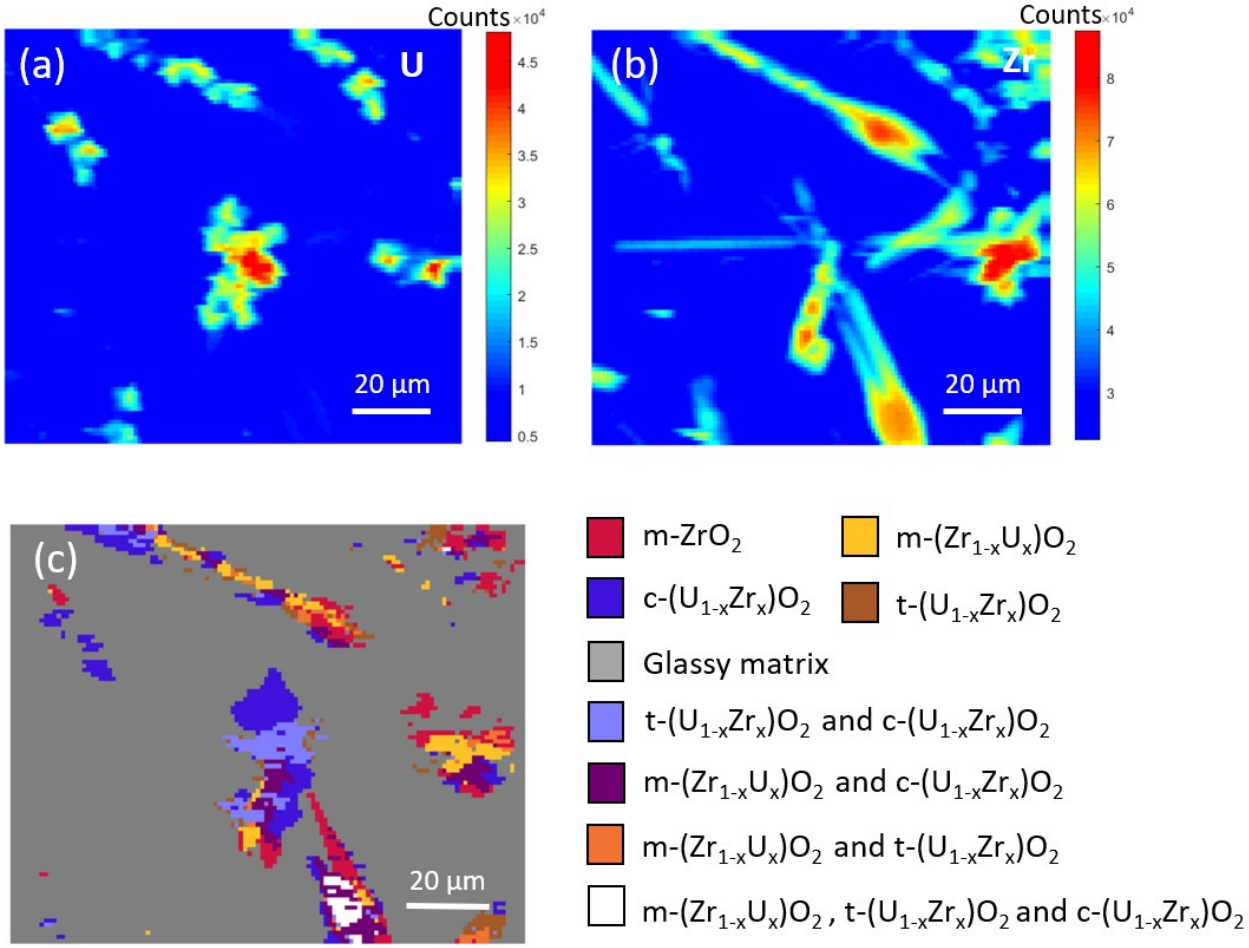

Supplementary Figure 2. Micro-focus analysis of simulant Black LFCM with a dendritic particle morphology. Figures **a – c** show the U-Lα, Zr-Kα and 2D µ-diffraction map reconstructed from XRD patterns for one representative region, respectively.

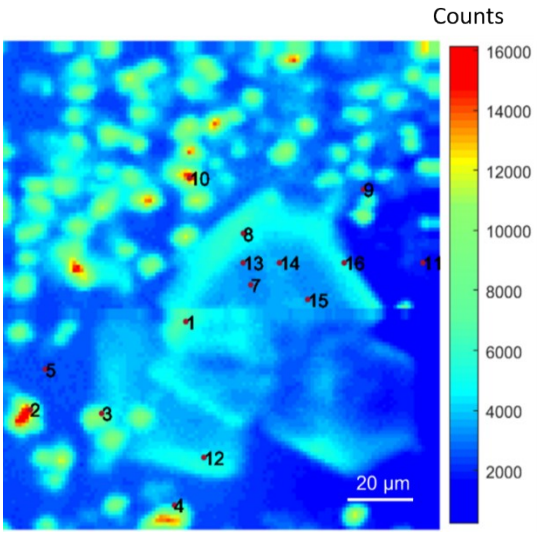

Supplementary Figure 3. U Lα µ-XRF map of simulant Brown LFCM, highlighting the positions of µ-XANES analysis.

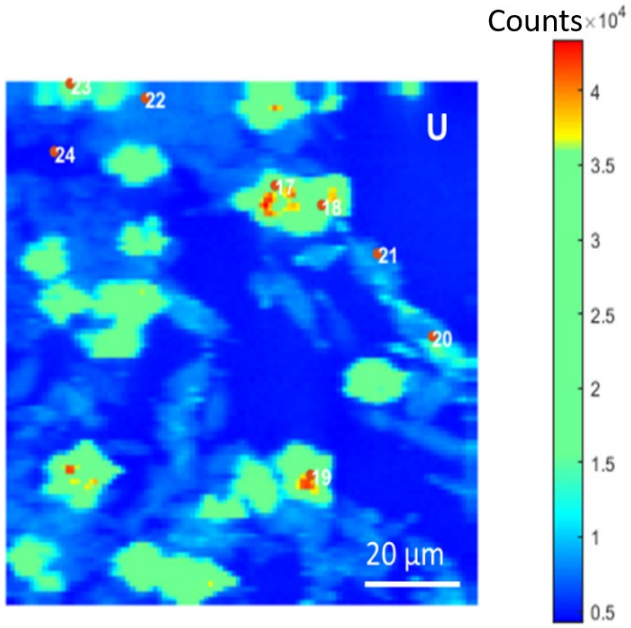

Supplementary Figure 4. U Lα µ-XRF map of simulant Black LFCM, highlighting the positions of µ-XANES analysis.

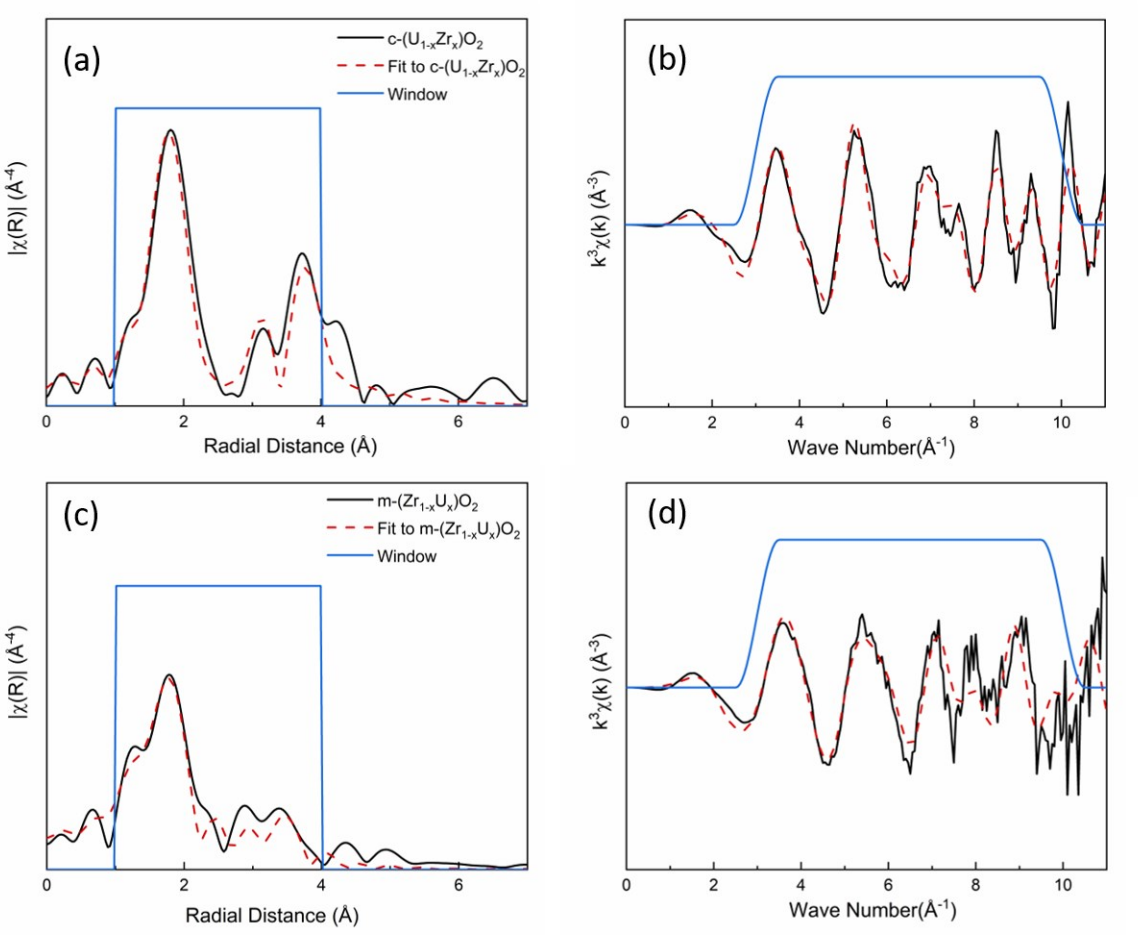

Supplementary Figure 5. Local coordination analysis of U in simulant LFCM by µ-EXAFS. Showing the spectra and model fit of **a** c-$(U_{1-x}Zr_x)O_2$ phase in Black LFCM µ-EXAFS spectrum in radial space ; **b** the corresponding k^3- weighted µ-EXAFS spectrum; **c** m-$(Zr_{1-x}U_x)O_2$ phase in Brown LFCM µ-EXAFS spectrum in radial space and **d** the corresponding k^3-weighted µ-EXAFS spectrum.

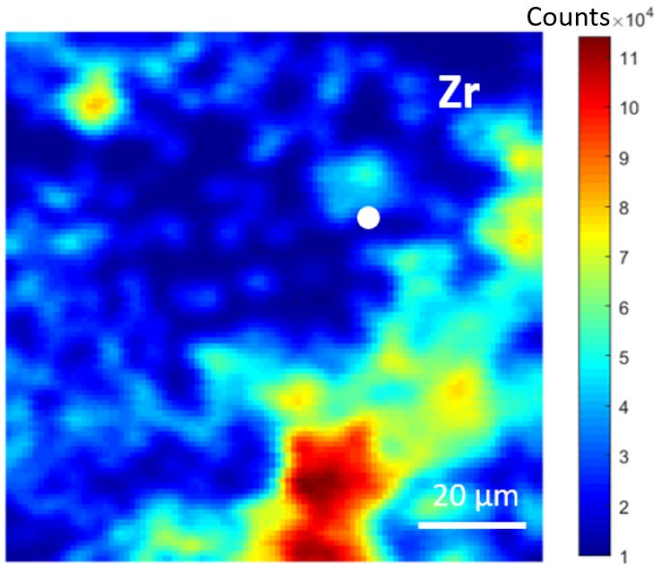

Supplementary Figure 6. Zr Kα µ-XRF map of simulant Brown LFCM, highlighting the position of µ-EXAFS analysis of glass.

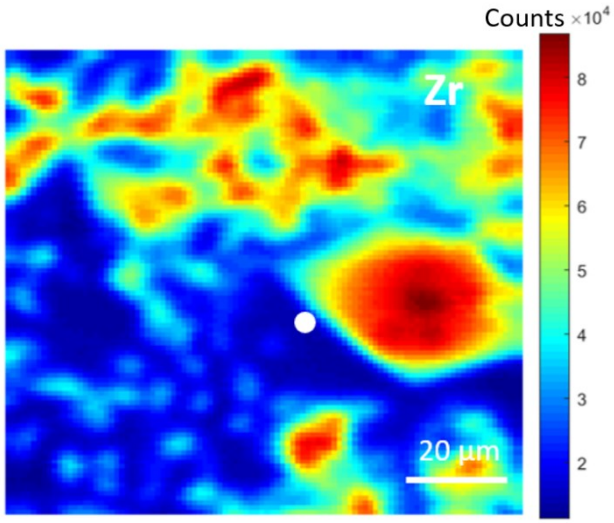

Supplementary Figure 7. Zr Kα µ-XRF map of simulant Black LFCM, highlighting the position of µ-EXAFS analysis of glass.

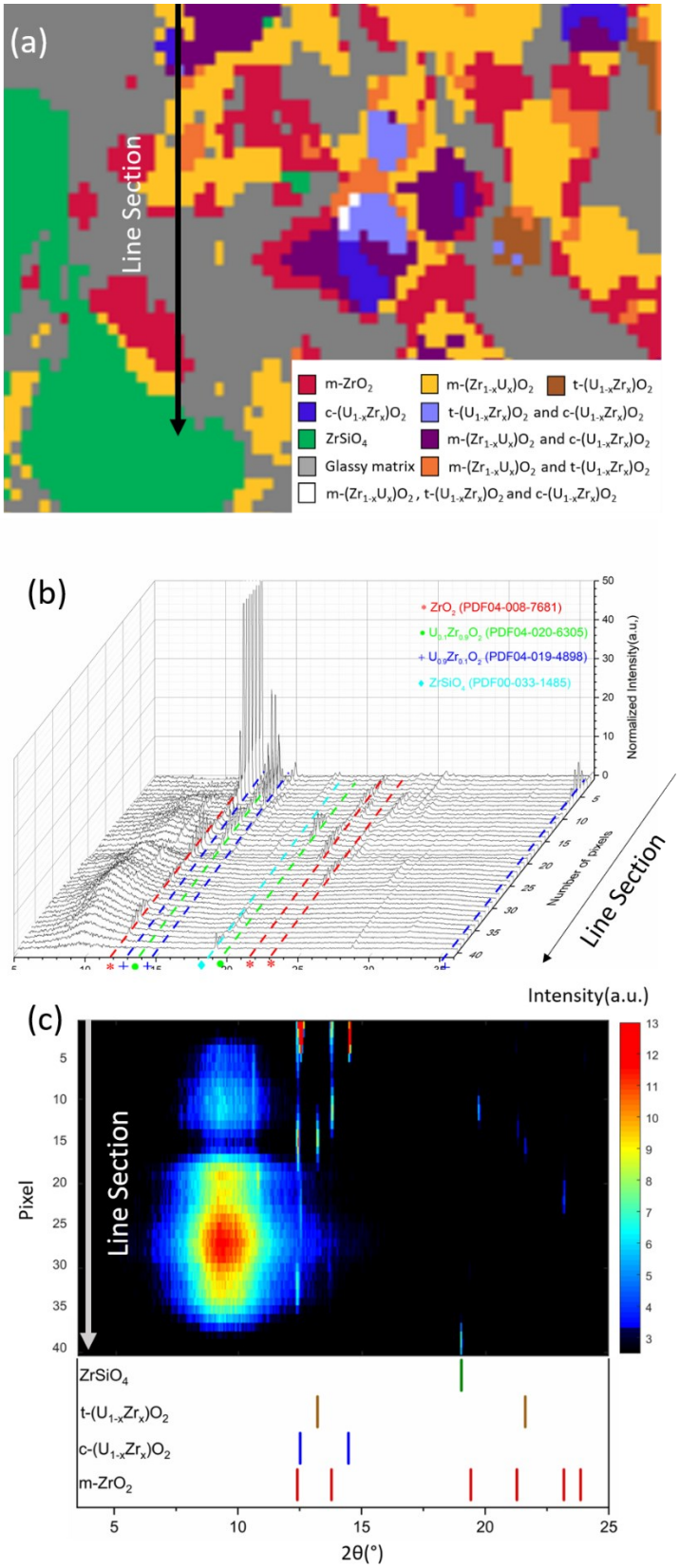

Supplementary Figure 8. The phase assemblage across a linear section of simulant Brown LFCM. **a** High magnification version of Figure 1(i), which is 2D μ-diffraction map highlighting the linear section and the phases it transects; **b** waterfall plot of μ-XRD patterns from each individual pixel across the linear section in **a**; and **c** 2D μ-XRD plot of the same data shown in b, highlighting the diffraction peak intensity (red is the highest intensity) and the 2θ positions of the reflections of the crystalline phases.

Supplementary Table 1. Compositions of simulant Brown and Black LFCM materials investigated.

Oxide component	Brown LFCM (mol. %)	Black LFCM (mol. %)
SiO_2	65.5	67.9
CaO	7.3	8.2
ZrO_2	3.3	3.0
Na_2O	5.3	5.8
BaO	0.1	0.1
Al_2O_3	4.2	5.1
MnO	0.5	0.4
Fe_2O_3	0.5	-
MgO	10.7	8.4
UO_2	2.5	1.2

Supplementary Table 2. μ-EXAFS fit parameters of crystalline phases in simulant Brown and Black LFCM. Since there monoclinic UO_2 does not exist, the m-$(Zr_{1-x}U_x)O_2$ was fitted with two U-O shells to simply represent the monoclinic structure.

				O-Shell				Si-Shell				
		S_O^2	R-factor	N1	U-O(Å)	$\sigma^2(10^{-2}Å^2)$	N2	U-Zr(Si)(Å)	$\sigma^2(10^{-2}Å^2)$	N3	U-U(Å)	$\sigma^2(10^{-2}Å^2)$
Brown LFCM	t-$(U_{1-x}Zr_x)O_2$	0.95	0.041	8	2.27 ± 0.02	1.03 ± 0.32	6.03 ±1.08	3.73 ± 0.03	0.89 ± 0.25	5.97 ±1.08	3.73 ±0.03	0.89 ± 0.25
Brown LFCM	c-$(U_{1-x}Zr_x)O_2$	0.95	0.027	8	2.32 ± 0.01	1.15 ± 0.10	3.24 ±1.17	3.83 ± 0.03	1.10 ± 0.28	8.76 ±1.17	3.83 ±0.03	1.10 ± 0.28
Brown LFCM	m-$(Zr_{1-x}U_x)O_2$	0.95	0.098	4	2.12 ±0.06	1.16 ± 0.83	8.88 ±2.44	3.91 ±0.36	1.29 ± 0.54	3.12 ±2.44	3.91 ±0.36	1.29 ± 0.54
				4	2.28 ±0.04	0.35 ± 0.43						
Black LFCM	c-$(U_{1-x}Zr_x)O_2$	0.95	0.028	8	2.32 ±0.01	1.19 ± 0.11	3.56 ±0.94	3.81 ±0.02	0.90 ± 0.20	8.44 ±0.94	3.81 ±0.02	0.90 ± 0.20
Black LFCM	$Zr_{1-x}U_xSiO_4$	0.95	0.033	4	2.26 ±0.11	1.04 ± 1.43	4	3.21 ±0.04	0.69 ± 0.57	4	3.81 ±0.05	1.00 ± 0.50
				4	2.36 ±0.13	1.04 ± 1.43	4	3.61 ±0.20	3.57 ± 3.82			

Supplementary Table 3. μ-EXAFS fit parameters of glass in simulant Brown and Black LFCM

			O-Shell						Si-Shell		
	S_O^2	R-factor	N1	U-O1(Å)	$\sigma^2(10^{-3}Å^2)$	N2	U-O1(Å)	$\sigma^2(10^{-3}Å^2)$	N3	U-Si1(Å)	$\sigma^2(10^{-3}Å^2)$
Brown LFCM	0.95	0.033	2.49 ±0.53	2.14 ±0.03	0.30 ± 3.00	3.98 ±1.05	2.32 ±0.03	0.30 ± 3.00			
Black LFCM	0.95	0.018	4.56 ±0.87	2.26 ±0.02	0.10 ± 3.00	3.36 ±0.57	2.45 ±0.02	0.10 ± 3.00	6.89 ±5.80	3.18 ±0.03	2.10± 1.40